JOURNAL OF PROPULSION AND POWER
Vol. 18, No. 1, January–February 2002

Active Control of Discrete-Frequency Noise Generated by Rotor–Stator Interactions

Scott Sawyer* and Sanford Fleeter†
Purdue University, West Lafayette, Indiana 47907
and
John Simonich‡
United Technologies Research Center, East Hartford, Connecticut 06108

Discrete-frequency tones generated by unsteady blade row interactions are of particular concern in the design of advanced turbine engines. In the annular fan inlet and exit duct, the acoustic waves generated at the multiples of the rotor blade pass frequency must have circumferential periodicity. The rotor–stator generated discrete-frequency noise is characterized as a summation of these circumferentially periodic acoustic waves or spatial modes over the multiples of the rotor blade pass frequency. Only the spatial modes that propagate to the far field represent the discrete-frequency noise received by an observer. A series of fundamental discrete-frequency noise source control experiments is described. Active airfoil source control is utilized to generate propagating spatial modes to interact with, and simultaneously cancel, the upstream and downstream propagating spatial modes generated by the rotor–stator interaction. The active airfoil source control is optimized for the control of the propagating spatial modes. The active noise control system incorporates the active airfoil source control with in-duct spatial mode measurements. Data are acquired and analyzed that demonstrate the viability of this unique active noise control technique. Significant simultaneous noise reductions are achieved for the upstream and downstream propagating spatial modes. The control system is successfully demonstrated over a range of rotor blade pass frequencies.

Nomenclature

A_∞	=	freestream speed of sound
k_θ	=	tangential wave number
$k_{\theta,\text{critical}}$	=	critical Nyquist mode
k_μ	=	eigenvalue
k_ξ	=	axial wave number
M	=	axial mean flow Mach number
N	=	number of microphones
N_{blades}	=	number of rotor blades
N_{vanes}	=	number of stator vanes
n	=	rotor harmonic
P	=	spatial transform of acoustic pressure
p	=	acoustic pressure
Q_μ	=	eigenvalue
r	=	radial coordinate
U_∞	=	mean axial velocity
v	=	stator index, 0, 1, . . . , N_{vanes}
x	=	axial direction
α	=	mean stator angle of attack
θ	=	circumferential coordinate
ξ	=	axial coordinate
Ω	=	rotor circular frequency
Ω_p	=	pressure pattern phase speed
ω	=	frequency, $n N_{\text{blades}} \Omega$

Received 17 June 2000; revision received 1 July 2001; accepted for publication 31 July 2001.

*Graduate Research Assistant, School of Mechanical Engineering. Member AIAA.
†McAllister Distinguished Professor, School of Mechanical Engineering. Fellow AIAA.
‡Senior Research Engineer. Member AIAA.

Introduction

IN the design of advanced gas-turbine engines, aeroacoustics is an increasingly important issue. In addition to meeting the long-term performance requirements of increased fuel efficiency, decreased weight, and improved reliability and maintainability while being competitively priced, engine certification requires meeting prevailing noise regulations, such as the U.S. Federal Air Regulation 36 Stage 3 rules that are to be implemented through the end of this decade. In addition, more stringent noise level guarantees are often required of the engine manufacturer by airlines to meet tougher local airport noise requirements. Also, there is a near certainty that more stringent stage 4 requirements will require an additional reduction of 5–10 effective perceived noise level-dB.

Figure 1 shows the primary noise sources for a high-bypass turbofan engine and a typical turbomachinery noise spectrum: the fan, the low-pressure or booster compressor, and the low-pressure turbine.[1,2] Their noise signatures include a broadband noise level, with large spikes or tones at multiples of the blade passing frequency. For subsonic fans, the acoustic spectrum discrete tones are usually 10–15 dB above the broadband level. The discrete-frequency tones are generated by periodic blade row unsteady aerodynamic interactions between adjacent blade rows. Namely, turbomachine blade rows are subject to spatially nonuniform inlet flowfields resulting from either potential or viscous wake interactions. Potential flow interactions result from variations in the pressure field associated with the blades of a given row and their effect on the blades of a neighboring row moving at a different rotational speed. This type of interaction is of concern when the axial spacing between neighboring blade rows is small or flow Mach numbers are high. Wake interactions result from the impingement of wakes shed by one or more upstream rows on the flow through a downstream blade row. This type of interaction can persist over considerable axial distances. Both of these interactions result in the generation of acoustic waves that may propagate unattenuated and also interact with other blade rows.

Current noise control and reduction methods for high-bypass turbofan engines usually are a combination of turbomachinery noise source control and suppression. Source control is accomplished by increasing axial spacing between adjacent blade rows and by selecting blade and vane number combinations to produce cutoff,

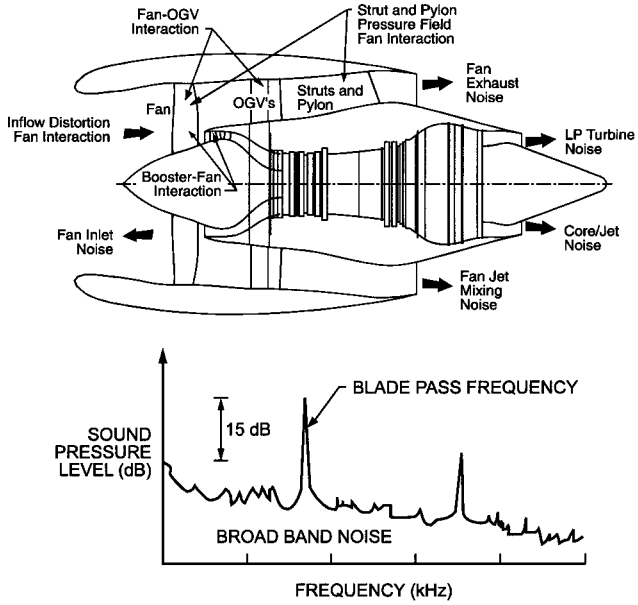

Fig. 1 Sources of turbomachine noise and the generated noise spectrum.

whereby the highest-energy acoustic modes decay exponentially with distance along the ducting. Source suppression is achieved with acoustic liners in the fan inlet and exhaust ducts and the core exhaust duct.

The increasing bypass ratios of advanced turbofan engines means increased fan diameter. However, nacelle length is to be kept at the current bypass ratio size, not scaled with diameter. Thus, inlet and exhaust duct length-to-diameter ratios will be smaller, and current liner design techniques will provide less noise suppression. Also, as the fan diameter increases, the blading becomes larger, and maintaining acoustically desired axial spacing becomes a severe weight penalty. Furthermore, the trend toward low blade number, wide-chord fan designs is a further deterrence to maintaining large spacing/chord ratios. Larger diameters, lower blade numbers, and lower tip speeds all produce lower blade passing frequencies that require deeper treatment liners to achieve comparable suppression. To provide low drag, however, large-diameter nacelles must be thin. As a result, current liner treatment designs will provide significantly less source suppression.

In summary, higher-bypass-ratio engines require more source noise control by design, not liner suppression, to even maintain current engine noise levels, let alone reduce noise levels significantly below those of current engines. As a result, progress in gas-turbine noise reduction is dependent on a better understanding of turbomachinery noise, specifically far-field discrete-frequency noise, and, after exhausting passive techniques, the designer is left to the active control of noise.

For a turbomachine stage, a rotor and stator in a duct, only specific circumferential acoustic modes are generated by the rotor–stator interactions, with these modes determined by the number of rotor blades and stator vanes. In addition, only certain of these modes propagate to the far field, with the rest decaying before reaching the far field. Thus, it is only those circumferential modes that propagate to the far field that represent the discrete-frequency noise received by an observer.

Active noise control has also been analytically modeled and experimentally demonstrated. Thomas et al.[3] applied a three-channel active control system to reduce fan noise radiating from the inlet of a JT15D turbofan engine. The error signals were provided by large-area microphones placed outside the inlet in the acoustic far field. The control sound field was generated by an array of 12 horns and 24 loudspeakers mounted on the circumference of the inlet. The control system utilized a feed-forward adaptive filtered least mean square algorithm. The 28-bladed rotor was excited by 28 rods mounted upstream of the rotor, which generated a plane wave spatial mode. With the three error microphones placed outside the engine, noise control was achieved within a 30-deg arc. However, there was an overall increase in the acoustic response.

Another approach to active noise control considers the reduction of the unsteady forces acting on the blade row.[4] This reduction in the unsteady lift translates into a decrease in noise generation. This was demonstrated by Simonich et al.[5] on an isolated airfoil with a moveable trailing-edge flap. The flap represented the active aerodynamic element of the system. The flap was actuated by a servomotor and its motion controlled to reduce the unsteady lift generated by a periodic disturbance. The peak-to-peak acoustic dipole pressure was reduced by a factor of two and the sound pressure level was reduced by 10 dB over portions of the spectrum.

A third approach combines the antinoise and source control techniques with the generation of antinoise at the noise source. This active airfoil source control technique minimizes power requirements and maximizes control authority. Kousen and Verdon[6] developed a computational model based on the linearized unsteady flow analysis LINFLO. The model considered blade surface mounted pistons as a source of antisound. Complete cancellation of all propagating waves required one surface actuator per acoustic wave. The amplitude and phase of the actuators were determined through the solution of a set of complex linear equations. Kousen[7] was also able to minimize the sound generation through a least-squares minimization procedure when the number of actuators was less than the number of propagating acoustic waves.

With on-airfoil source control and in-duct spatial mode measurements, both Minter et al.[8] and McCarthy and Fleeter[9] demonstrated active control of propagating spatial modes generated by a 16-bladed rotor and a 3-vaned stator. Amplitude and phase control was provided by three Ariel DSP-16 digital signal processing boards mounted in two PC compatible personal computers with input provided by a filtered 16-pulse transistor–transistor logic output of an optical encoder. Minter et al.[8] used piezoelectric crystals to actuate airfoil surface pistons and oscillating flaps to realize maximum noise reductions of 6 dB upstream and 8 dB downstream. McCarthy and Fleeter[9] used a compression driver–horn combination in a speaker–dipole arrangement for near source control of either the upstream or the downstream going acoustic wave. Maximum reductions of 17.1 dB upstream and 15 dB downstream were obtained.

This paper is directed at the reduction of discrete-frequency noise generated by rotor–stator interaction through a series of fundamental experiments performed in the Purdue Rotating Annular Cascade Research Facility. The active discrete-frequency noise control system combines the advantages of on-airfoil active source control with in-duct acoustic measurement for the simultaneous cancellation or reduction of a rotor–stator generated spatial mode propagating upstream and downstream. This unique active discrete-frequency noise control system is optimized for the control of rotor–stator generated propagating spatial modes over a wide range of operating conditions.

Discrete-Frequency Noise Generation and Control

The classical model of discrete-frequency noise in a turbomachine considers a rotor and stator in an annular duct.[10] For example, in a multistage turbomachine unsteady pressure is generated on stator rows due to the periodic wakes of an upstream rotor blade row and the potential fields of upstream and downstream rotor blade rows. These unsteady stator vane surface pressures are the source of turbomachine discrete-frequency noise. The stator row responds to these periodic excitations by generating fluctuating periodic lift forces at multiples of the rotor blade pass frequency. This stator row unsteady loading then couples to the duct to produce acoustic waves.

The acoustic response of the stator row is characterized as the superposition of spatial modes, where the generated spatial modes are a function of the number of rotor blades and the number of stator vanes. A spatial mode is described as a lobed pressure pattern where the spatial mode order is equal to the number of lobes. The propagation, resonance, or decay of a spatial mode is given by the axial wave number. Of the generated modes, only certain modes propagate to the far field. It is these propagating modes that represent the discrete-frequency noise received by an observer. These acoustic response characteristics are important to explain properly the measured acoustic response due to rotor–stator interactions and

to provide the necessary understanding of the basic concepts of an active discrete-frequency noise control system.

Annular Duct Acoustics

The unsteady flow in an annular duct is described by the wave equation for a uniform axial flow, derived by considering the flow to be inviscid and compressible with small unsteady perturbations:

$$\left(\frac{\partial}{\partial t}+U_\infty\frac{\partial}{\partial \xi}\right)^2 p = A_\infty^2\left[\frac{1}{r}\frac{\partial}{\partial r}\left(r\frac{\partial}{\partial r}\right)+\frac{1}{r^2}\frac{\partial^2}{\partial \theta^2}+\frac{\partial^2}{\partial \xi^2}\right]p \tag{1}$$

where p is the acoustic pressure; A_∞ is the freestream speed of sound; U_∞ is the freestream axial velocity; and ξ, r, and θ are the axial, radial, and circumferential coordinates.

The acoustic pressure is a function of radius and is harmonic in time, axial distance, and polar angle:

$$p(\xi, r, \theta, t) = \bar{p}(k_\mu r)\exp[i(k_\xi \xi + k_\theta \theta - nN_{\text{blades}}\Omega t)] \tag{2}$$

where $\omega = nN_{\text{blades}}\ \Omega$ is a multiple of blade passage frequency; n is the rotor harmonic; the spatial mode order $k_\theta = nN_{\text{blades}} + mN_{\text{vanes}}$ is determined to satisfy stator vane row periodicity conditions; $m = 0, \pm 1, \pm 2, \ldots$, is an arbitrary integer; the radial variation of the pressure is described by $\bar{p}(k_\mu r) = J_{k_\theta}(k_\mu r) + Q_\mu Y_{k_\theta}(k_\mu r)$; a combination of Bessel functions of order k_θ, k_μ, and Q_μ are the eigenvalues determined from the flow tangency conditions at the inner and outer duct radii:

$$k_\xi = \frac{k_\omega M}{1-M^2} \pm \sqrt{\left(\frac{k_\omega M}{1-M^2}\right)^2 + \frac{k_\omega^2 - k_\mu^2}{1-M^2}}$$

the axial wave number, is determined through the solution of the characteristic equation, $k_\omega = \omega/A_\infty$; and M is the Mach number of the freestream flow.

Far-Field Discrete-Frequency Noise

Although an infinite number of spatial modes are generated by the rotor–stator interaction at the harmonics of blade passage frequency, only certain of these modes propagate to the far field, with the rest decaying before reaching the far field. Thus, it is only those spatial modes that propagate to the far field that represent the discrete-frequency noise received by an observer. The propagation of the acoustic pressure modes is specified by the axial dependence of the duct pressure waves, that is, the axial wave number, specifically the expression under the radical of

$$k_\xi = \frac{k_\omega M}{1-M^2} \pm \sqrt{\left(\frac{k_\omega M}{1-M^2}\right)^2 + \frac{k_\omega^2 - k_\mu^2}{1-M^2}} \tag{3}$$

where for $k_\omega^2 - k_\mu^2(1-M^2) > 0$ there are two real k_ξ values corresponding to two propagating pressure waves, one upstream and the other downstream. For $k_\omega^2 - k_\mu^2(1-M^2) < 0$ there are two complex k_ξ values corresponding to two decaying waves, one upstream and the other downstream. The case of $K_\omega^2 - K_\mu^2(1-M^2) = 0$ is a resonance condition, with the resonant frequency known as the cutoff frequency because below the cutoff frequency the pressure waves decay in the axial direction or are cutoff.

Experimental Facility and Instrumentation

The experiments were performed in the Purdue Rotating Annular Cascade Research Facility (Fig. 2). This facility is an open-loop draw through type wind tunnel capable of test section velocities of 220 ft/s (67.06 m/s). The flow, conditioned by a honeycomb section and an acoustically treated inlet plenum, accelerates though a bellmouth inlet to the constant area annular test section. The flow exiting the test section is diffused into a large acoustically treated exit plenum. The flow is drawn through the facility by a 300-hp (223.7 kW) centrifugal fan located downstream of the exit plenum.

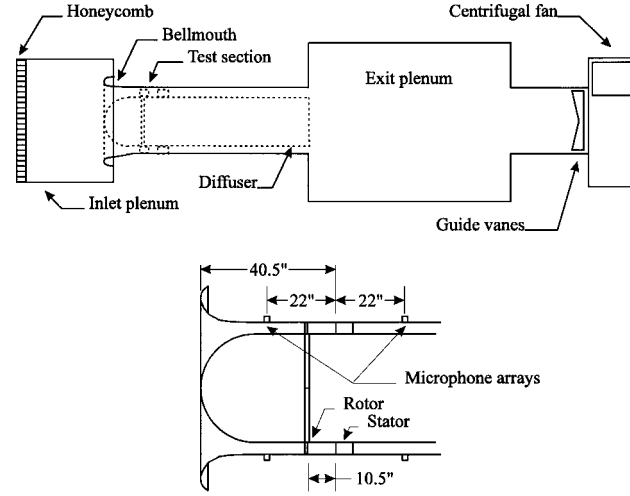

Fig. 2 Purdue annular cascade facility.

Two arrays of 10 Piezotronics, Inc., PCB 103A piezoelectric microphones with uniform circumferential spacing are mounted by static pressure taps in the outer wall of the inlet annulus (Fig. 2).

The microphones have a nominal sensitivity of 1500 mV/psi (188.57 mV/kPa) and a natural frequency of 13 kHz. The microphones are calibrated as installed in the rig and show linear amplitude response and flat frequency response in the region of interest. Experimental error in the pressure measurement is within 3% amplitude and 5-deg phase. The Nyquist critical mode $k_{\theta,\text{critical}}$ is 5 for the 10-microphone array, with all spatial modes above the Nyquist critical mode aliased below the Nyquist mode.

The annular test section was configured with a rotor with 16, 1-in.-wide perforated plates upstream of a stator with 18 NACA 65A012 airfoils with a 15.24 cm (6.00 in.) chord. An optical pickup on the rotor shaft was utilized to determine the rotor shaft speed.

The 16 rotor blades and 18 stator vanes in the test section generate $k_\theta = n16 + m18$ spatial modes, where n is the rotor harmonic and m is an arbitrary integer. Therefore, the spatial modes $k_\theta = \ldots, -20, -2, 16, \ldots$, are generated at blade pass frequency. At twice blade pass frequency, the spatial modes $k_\theta = \ldots, -22, -4, 14, \ldots$, are generated by the rotor–stator interaction. For operating conditions from 800 to 1000 rpm, only the $k_\theta = -2$ mode is cut on at blade pass frequency, and the $k_\theta = -4$ at twice blade pass frequency are cut on and generated by the rotor–stator interaction. The interblade phase angle of the 16-bladed rotor and the 18-vaned stator is -320 deg.

Active Discrete-Frequency Noise Control

The far-field discrete-frequency noise of a turbomachine received by an observer is composed of spatial modes generated at multiples of rotor blade pass frequency that have propagated in the duct and have radiated to the acoustic far field. These discrete-frequency tones are generated by rotor–stator interactions and can be characterized through the measurement of the modal structure in the duct both upstream and downstream of the airfoil rows. The function of the active noise control system is the cancellation or reduction of the propagating acoustic modes in the duct, that is, before the modes are radiated to the far field. The active noise control system utilizes active airfoil source control that mimics the rotor–stator interaction and is optimized for control of the propagating acoustic modes generated by the rotor–stator interaction. Additionally, on-airfoil actuators minimize the actuator power requirements.

An acoustic wave generated by rotor–stator interaction is characterized by the spatial modes and the excitation frequency. The spatial modes generated are specified by the number of rotor blades and stator vanes $k_\theta = nN_{\text{blades}} + mN_{\text{vanes}}$. Ideally, the active control system and the rotor–stator interaction produce the same propagating acoustic waves. This enables the active control system to cancel the rotor–stator generated propagating waves, resulting in no discrete-frequency noise in the far field. The interaction of a 16-blade rotor

and an 18-vaned stator generates a $k_\theta = -2$ propagating spatial mode at blade pass frequency. The stator equipped with active source control also generates a $k_\theta = -2$ propagating spatial mode at blade pass frequency. If the noise generated by the active source control is out of phase with the noise generated by the rotor–stator interaction, the result is complete cancellation of the discrete-frequency noise in the duct.

The source of the discrete-frequency noise is the unsteady loading on the stator airfoils, with the unsteady loading of adjacent airfoils equal in magnitude and shifted in phase by the interblade phase angle. The active noise control system is realized by placing an acoustic source on each stator vane. When successive acoustic sources are driven on adjacent stator vanes by signals that are equal in magnitude and shifted in phase by the interblade phase angle, the acoustic sources and the rotor–stator interactions generate the same spatial modes (Fig. 3). The spatial modes generated by the acoustic sources will propagate or decay upstream and downstream in the same manner as the spatial modes generated by the rotor–stator interactions.

For example, a 16-bladed rotor interacting with an 18-vaned stator generates the $k_\theta = \ldots, -20, -2, 16, \ldots,$ spatial modes at blade pass frequency. At 1000 rotor shaft rpm, only the $k_\theta = -2$ mode propagates to the far field. The spatial modes propagating upstream and downstream are characterized by the complex amplitudes $P_{\text{gust,up}}(k_\theta = -2)$ and $P_{\text{gust,down}}(k_\theta = -2)$. It is these modes that will be canceled through active control, as illustrated in Fig. 4. The control system is assumed to be linear with the control signal input amplitude. Therefore, the active control system is characterized by the generated complex amplitudes $P_{A_1,\text{up}}(k_\theta = -2)A_1$ and $P_{A_1,\text{down}}(k_\theta = -2)A_1$, where $P_{A_1,\text{up}}(k_\theta = -2)$ and $P_{A_1,\text{down}}(k_\theta = -2)$ are the influence coefficients generated by the actuators and A_1 is the complex amplitude of the control signal.

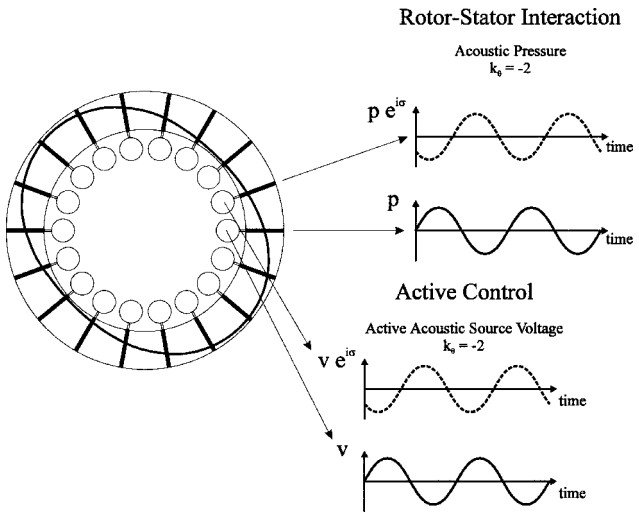

Fig. 3 Vane-to-vane phase shift of acoustic pressure and active control voltage.

Thus, the amplitude and phase of the source control signal can be set to reduce the upstream or the downstream propagating mode, but not both at the same time. The simultaneous reduction of one propagating spatial mode both upstream and downstream of the blade rows requires two sets of acoustic sources. The measured response is simply expressed in matrix form

$$\begin{bmatrix} P_{A_1,\text{up}} & P_{A_2,\text{up}} \\ P_{A_1,\text{down}} & P_{A_2,\text{down}} \end{bmatrix} \begin{bmatrix} A_1 \\ A_2 \end{bmatrix} = \begin{bmatrix} P_{\text{measured,up}} & -P_{\text{gust,up}} \\ P_{\text{measured,down}} & -P_{\text{gust,down}} \end{bmatrix} \quad (4)$$

where $P_{A_2,\text{up}}$ and $P_{A_2,\text{down}}$ are the influence coefficients of the second set of acoustic drivers and A_2 is the complex amplitude of the second control signal.

For zero measured response, Eq. (4) becomes

$$\begin{bmatrix} P_{A_1,\text{up}} & P_{A_2,\text{up}} \\ P_{A_1,\text{down}} & P_{A_2,\text{down}} \end{bmatrix} \begin{bmatrix} A_1 \\ A_2 \end{bmatrix} = \begin{bmatrix} -P_{\text{gust,up}} \\ -P_{\text{gust,down}} \end{bmatrix} \quad (5)$$

The required control signals are

$$\begin{bmatrix} A_1 \\ A_2 \end{bmatrix} = \begin{bmatrix} P_{A_1,\text{up}} & P_{A_2,\text{up}} \\ P_{A_1,\text{down}} & P_{A_2,\text{down}} \end{bmatrix}^{-1} \begin{bmatrix} -P_{\text{gust,up}} \\ -P_{\text{gust,down}} \end{bmatrix}$$

To reiterate, the simultaneous cancellation of one rotor–stator interaction generated propagating spatial mode $P_{\text{gust,up}}$ and $P_{\text{gust,down}}$ both upstream and downstream of the airfoil rows requires two sets of acoustic sources. Each set of acoustic sources will produce upstream and downstream going spatial modes. When each set of acoustic sources is driven at the proper amplitude and phase, cancellation of both propagating waves is possible. The measured acoustic pressure of the propagating mode is equal to the superposition of the rotor–stator noise with that due to the active control system.

Active Airfoil Source Control

The central component of this active noise control system is the active stator airfoils that generate propagating spatial modes analogous to those of the rotor–stator interaction. The acoustic sources are driven at the excitation frequency and have the same phase shift from stator vane to stator vane. Thus, the active control system mimics the rotor–stator interaction and generates a $k_\theta = -2$ spatial mode.

The twin-cavity active airfoil with perforated metal sheathing is shown in Fig. 5. The cavity access ports located on the airfoil hub allow the airfoil to be driven by a remote centerbody-mounted acoustic source. The microperforated sheathing minimizes the disturbance of the stator vane aerodynamics while providing only minor resistance to the acoustic radiation from the cavity. The perforated screen has 0.010-in.-diam holes and a 30% open area.

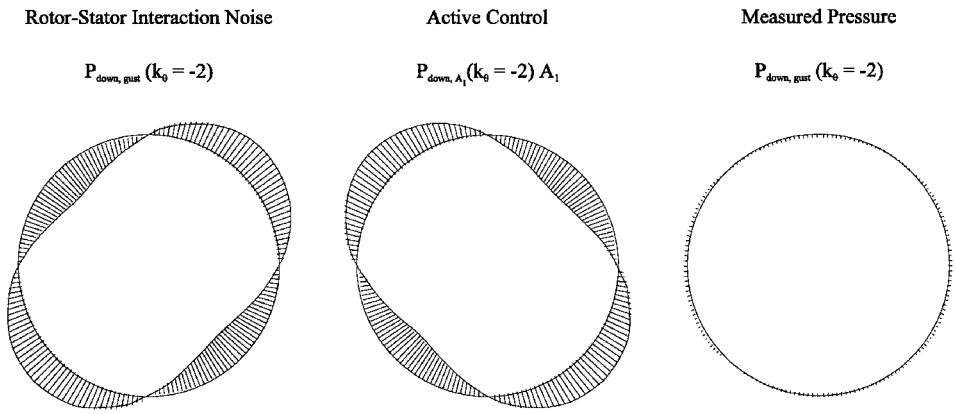

Fig. 4 Active control of $k_\theta = -2$ mode in the downstream duct.

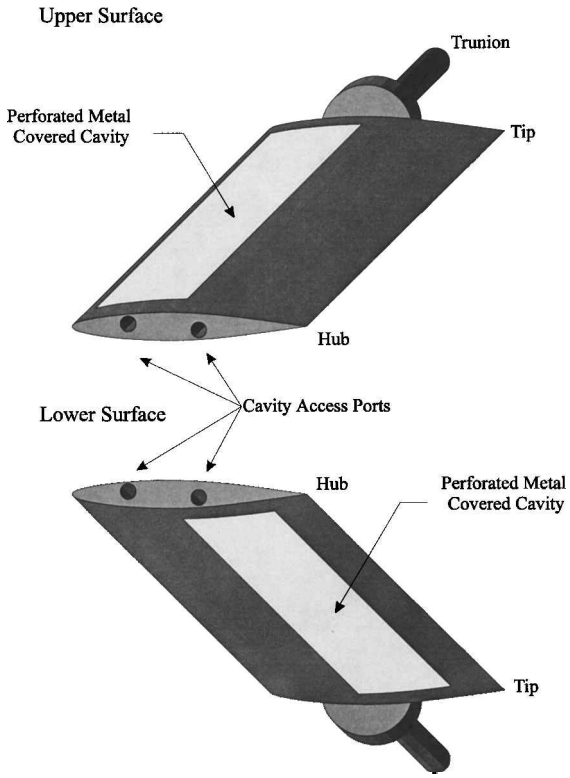

Fig. 5 Active stator airfoil.

The dimensions of the connector and vane cavity were selected such that the cavity and the tube formed a resonator tuned to the rotor blade pass frequency at 1000 rotor shaft rpm (267 Hz). This resonator configuration provided an amplification of 12 dB relative to the compression driver alone. This configuration is also characterized by a sufficiently broad bandwidth that was necessary to achieve a useful operating range specified for the experiments.

Both the upper- and lower-surface actuators generate upstream and downstream going propagating spatial modes. When the two sets of actuators are driven in concert by signals of proper amplitude and phase, the active airfoils of the stator vane row cancel the upstream and downstream propagating spatial modes.

The active control system is set up to naturally mimic the rotor–stator interaction noise, with the physics that govern the rotor–stator interactions also applying to the active noise control system. The control signal generation is characterized by the magnitude and phase of two reference signals. The reference signals drive the zeroth stator vane of the cascade, with successive stator vanes driven by the same magnitude signal shifted in phase by the interblade phase angle. The amplitude and phase of the reference signals are set to reduce the measured propagating acoustic wave both upstream and downstream of the rotor–stator.

The generation of the control signals is accomplished using three Computer Boards, Inc., model CIO DDA06 six-channel analog output boards installed in a PC compatible computer. The digital-to-analog converters are programmed to produce sinusoidal output signals at blade pass frequency and are phase referenced to the output of the optical rotor–shaft encoder. The generation of the proper spatial mode is ensured because interblade phase angle is set to the value determined by the rotor–stator interaction. The signal generation rate and phase reference are performed in real time. The control signals drive the compression drivers via Kenwood KM-X1 surround-soundpower amplifiers and transformers to match the amplifier output impedance to the impedance provided by the compression drivers.

Data Acquisition and Signal Processing

Acquisition and digitization of the microphone signals and the shaft trigger signal is accomplished using five National Instruments NB-A2000 analog-to-digital boards installed in an Apple Macintosh Quadra 950 computer. This system allows the simultaneous acquisition of 20 channels of data, initiated by the shaft trigger signal. Ensemble averaging over 100 rotor revolutions is utilized to reduce the random noise not linked to the rotor passage.

A primary component of the active noise control system is the measurement of the propagating spatial modes[11,12] generated by both the rotor–stator interaction and the active airfoil source control system. The measured spatial modes not only characterize the baseline rotor–stator response, but also quantify the effectiveness of the active noise control system.

The discrete-frequency acoustic response is the superposition of spatial modes generated at the multiples of rotor blade pass frequency, with the acoustic modes at blade pass and twice blade pass frequency being of primary concern. An array of microphones is required to determine the measured acoustic response as a function of both frequency and spatial mode. This temporal-spatial transform is accomplished using two discrete Fourier transforms. The first determines the frequency content of the microphone signals, and the second determines the amplitude of spatial modes at each frequency. The spatial transform, operating on the temporal Fourier transform, is a function of frequency that separates the forward and backward spinning modes. Note that the measurement errors are estimated to be less than 5%. Based on a 95% confidence level, the maximum estimated error on the mean is 3%.

Results

To demonstrate the viability and the effectiveness of this discrete-frequency active noise control system, a series of experiments was performed in the Purdue Rotating Annular Cascade Research Facility. A rotor with 16 perforated plates upstream of a stator with 18 active symmetric airfoils was installed in the annular test section, with circumferential arrays of microphones in the inlet and outlet used for spatial mode measurement. Rotor shaft rotation was varied from 800 to 1000 rpm, and the axial velocity was 85 ft/s. At blade pass frequency, the $k_\theta = -2$ spatial mode propagates both upstream and downstream. Because the $k_\theta = -2$ spatial mode represents the discrete-frequency noise produced by the rotor–stator interaction, the control system was designed to minimize the amplitude of that spatial mode.

The effectiveness of the control system is seen in Fig. 6 where the upstream and downstream modal amplitudes are shown for the baseline rotor–stator interaction and the simultaneous upstream and downstream active control. Noise reductions of nearly 20 dB upstream and over 20 dB downstream are realized.

Figure 7 shows the controlled and the uncontrolled amplitudes of the $k_\theta = -2$ spatial mode as a function of rotor shaft rotation, with simultaneous control of the $k_\theta = -2$ spatial mode both upstream and downstream of the rotor–stator. Significant control

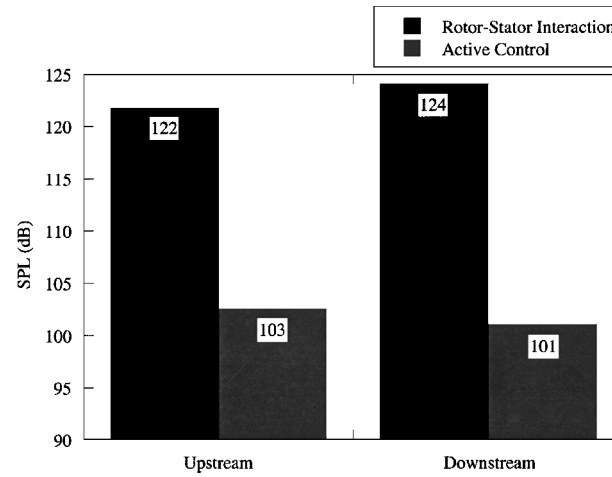

Fig. 6 Simultaneous upstream and downstream control.

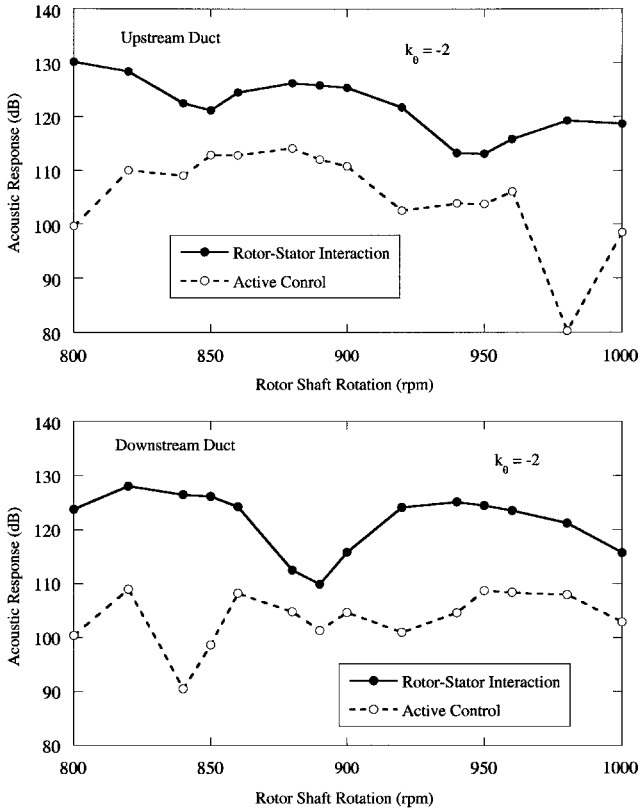

Fig. 7 Simultaneous control of upstream and downstream propagating discrete-frequency noise.

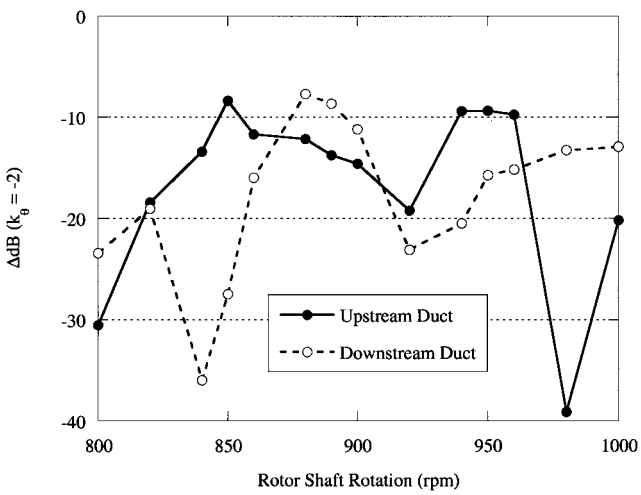

Fig. 8 Control authority demonstrated over a large range of operating conditions.

authority was demonstrated over the entire range of operating conditions.

Figure 8 shows the reduction of the generated discrete-frequency noise relative to the noise generated by the rotor–stator interaction. Reductions of over 10 dB were achieved over nearly the entire range of operating conditions, and maximum reductions of 30–40 dB were demonstrated for certain conditions.

Figure 9 shows the amplitude and phase of the control signals required to realize the simultaneous control of the upstream and downstream propagating discrete-frequency noise as a function of rotor shaft rotation. Fortunately, the required control signals were nearly in phase and of comparable amplitude. This situation allows the drivers to complement each other and represents the minimum power consumption of the system.

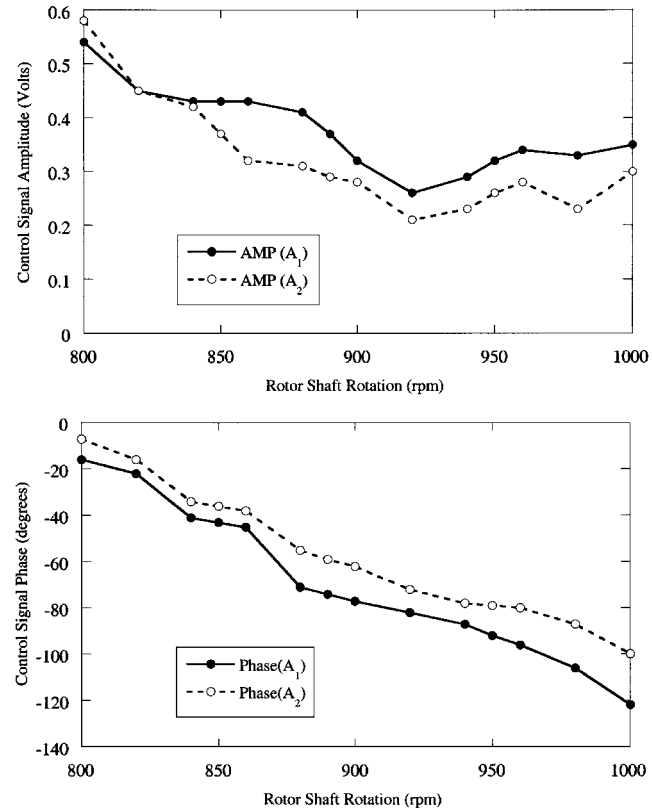

Fig. 9 Control signal voltage amplitude and phase as a function of rotor shaft rotation.

Summary

Advanced-design high-bypass turbomachines generate prominent discrete-frequency tones. These tones are generated by rotor–stator interactions, with specific spatial modes generated. However, only certain of these generated modes propagate to the far field, with these representing the far-field discrete-frequency noise. High-bypass turbomachines limit the effectiveness of current state-of-the-art acoustic treatments for suppression and source control. As prevailing noise regulations become ever more stringent, innovative control of turbomachine noise sources is increasingly important. Thus, a series of fundamental experiments was performed to demonstrate the effectiveness of active simultaneous control of upstream and downstream propagating discrete-frequency noise using active airfoil source control.

In the active airfoil source control technique, the upstream and downstream propagating modes, that is, the far-field tone noise, are simultaneously canceled through the generation of control propagating waves that interact with and cancel those modes generated by the rotor–stator interaction. The active airfoil source control is optimized for the control of propagating spatial modes. The active noise control system incorporates active airfoil source control with in-duct spatial mode measurements and real-time rotor phase referenced control signal generation.

The active airfoil source control system was successfully demonstrated over a wide range of operating conditions with simultaneous reductions of 10 dB realized over most of the operating range. In some cases, nearly 40 dB of control authority was demonstrated.

Acknowledgments

This research was sponsored in part by NASA John H. Glenn Research Center at Lewis Field. The technical interactions with Daniel Buffum and Laurence J. Heidelberg, as well as the financial support, are most gratefully acknowledged.

References

[1] Gliebe, P. R., "Aeroacoustics in Turbomachines and Propellers—Future Research Needs," *Proceedings of the 6th International Symposium on Unsteady Aerodynamics, Aeroacoustics, and Aeroelasticity of Turbomachines*

and Propellers, edited by H. F. Atassi, Springer-Verlag, New York, 1992, pp. 619–642.

[2]Groeneweg, J. F., and Rice, E. J., "Aircraft Turbofan Noise," *Journal of Turbomachinery*, Vol. 109, No. 1, 1987, pp. 130–141.

[3]Thomas, R. H., Burdisso, R. A., Fuller, C. R., and O'Brien, W. F., "Preliminary Experiments on Active Control of Fan Noise from a JT15D Turbofan Engine," *Journal of Sound and Vibration*, Vol. 161, No. 3, 1993, pp. 532–537.

[4]Goldstein, M., *Aeroacoustics*, McGraw–Hill, New York, 1975, pp. 189–215.

[5]Simonich, J., Lavrich, P., Sofrin, T., and Topal, D., "Active Aerodynamic Control of Wake–Airfoil Interaction Noise-Experiment," *AIAA Journal*, Vol. 31, No. 10, 1993, pp. 1761–1768.

[6]Kousen, K. A., and Verdon, J. M., "Active Control of Wake/Blade Row Interaction Noise," *AIAA Journal*, Vol. 32, No. 10, 1994, pp. 1953–1960.

[7]Kousen, K. A., "Multiple Mode Minimization of Wake/Blade–Row Interaction Noise Using a Single Actuator Per Blade," AIAA Paper 96-1691, Oct. 1993.

[8]Minter, J. A., Hoyniak, D., and Fleeter, S., "Active Airfoil Surface Control of Wake-Generated Discrete-Frequency Noise," AIAA Paper 94-2952, June 1994.

[9]McCarthy, S. M., and Fleeter, S., "Dipole Active Control of Wake–Blade Row Interaction Noise," AIAA Paper 96-1783, May 1996.

[10]Tyler, J. M., and Sofrin, T. G., "Axial Flow Compressor Noise Studies," *SAE Transactions*, Vol. 70, 1962, pp. 309–332.

[11]Sawyer, S., and Fleeter, S., "Mean Stator Loading Effect on the Acoustic Response of a Rotating Cascade," AIAA Paper 94-2953, June 1994.

[12]Sawyer, S., Feiereisen, J. M., and Fleeter, S., "Influence of Rotor Detuning on the Acoustic Response of an Annular Cascade," AIAA Paper 96-1689, May 1996.